ONLINE MONITORING OF ALUMINIUM PRIMARY PRODUCTION GAS COMPOSITION BY USE OF FOURIER-TRANSFORM INFRARED SPECTROMETRY

Thor A. Aarhaug[1], Alain Ferber[2], Ole Kjos[1] and Heiko Gaertner[3]
[1]SINTEF Materials and Chemistry, 7465 Trondheim, Norway
[2]SINTEF Information and Materials Technology, 0324 Oslo, Norway
[3]NTNU, Department of Materials Science and Engineering, 7491 Trondheim, Norway
Keywords: Gas analysis, FTIR, calibration, quantitation

Abstract

Online monitoring of aluminium primary production raw gas is challenging due to the high concentration of HF in the presence of water. Tunable Diode Laser (TDL) analyzers retrofitted with sapphire optical windows allow for online monitoring of raw gas composistion. These systems are however limited to one or two gas constituents. In order to make use of multi-component analyzers like Fourier-Transform InfraRed Spectrometers (FTIR), HF must be selectively removed by filtration. This work presents some results from complete mapping of raw gas composition by comparing results from HF filtrated as well as non-filtrated measurements. The multivariate calibration models established for mapping of the raw gas is discussed. Open-path FTIR spectroscopy was applied in order to quantify fugitive emissions of HF and SO2. Quantitation showed good correlation with reported emissions. Monitoring of fugitive PFC emissions was also evaluated.

Introduction

Knowledge of the primary aluminium raw gas composition is important when aiming at reducing energy consumption of the primary metal production. Introduction of heat exchangers in the raw gas faces challenges like corrosion and scaling. As heat exchangers benefit from a higher raw gas temperature, a more concentrated raw gas would be the result. The reduced energy input to fan power is substantial [1]. Although the formation of scale is still poorly understood [2, 3], it is plausible that the water content of the raw gas is of importance. The main obstacle for online monitoring of raw gas composition is the presence of HF and water. Whereas Tunable Diode Lasers (TDL) can be retrofitted with IR transmitting sapphire optical windows, Fourier-Transform InfraRed (FTIR) spectrometers makes use of gold-plated mirrors that are subject to corrosion. Selective removal of HF from the gas is difficult to achieve. Monitoring of gas composition downstream the dry scrubber is, after removal of particles, straightforward. Some losses in concentration of species like COS and SO_2 in addition to water is observed. For monitoring of labile gas species in the raw gas, direct analysis of the raw gas is required. For this purpose, an IR light path can be set up across the raw gas exhaust pipe. Alternatively, the beam can be set up across or through an electrolysis cell.

Multicomponent gas analysers are generally more complex in operation and calibration than single component analysers. For complex gas mixtures, a multivariate approach to quantitation is required. The computing power of today's desktop computers sets few limitations to the choice in spectral decomposition technique. One of the most powerful techniques for complex gas mixtures is Partial Least Squares Regression (PLSR). Instead of regressing spectral data against concentration data in a separate step, PLS uses the concentration data during the decomposition process. In this way, the concentration data is weighted. PLS allows for calibration of only gas constituents of interest, thus a few constituents in a complex gas mixture can be quantified. PLS calibration models for FTIR with predictive capabilities can be computed with MATLAB, preferably with a statistics toolbox. For incorporation into FTIR instrument for direct concentration readout, dedicated software for model building if probably more efficient. If not FTIR vendor provide PLS model capabilities, Grams IQ [4] provides versatile export capabilities.

In this work, the application of potassium hydroxide impregnated filters was evaluated as a method for online monitoring of raw gas composition with FTIR. The filter performance was evaluated by comparison with burst, unfiltered measurements of the raw gas. Labile gas species in the raw gas was evaluated by Open Path FTIR spectroscopy. The same technique was used to evaluate fugitive emission (roofing). FTIR quantitation was performed by the establishment of a PLS-1 multivariate model for the raw gas. The model performance was evaluated by manual calculations as comparison with other models.

Experimental

For extractive gas analysis a Protea LTD ProtIR 204 M process analyser was applied. The instrument specifics include a 6.4 meter path gas cell and an apparent resolution of 1 cm^{-1}. For direct gas measurements, an ABB MR170 spectrometer with stirling cooled detector was used. The ProtIR instrument comes with a quantitation model that complies with BS EN 14181 standard for monitoring of stationary emissions. A custom model for primary aluminium production was ordered from Protea LTD. The specifications given for the gas are shown in Table 1.

Table 1. Raw gas specification for the quantitation model. SF6 was added for gas tracer capabilities. CO_2 and water concentrations were exaggerated for other purposes.

Compound	Typical concentration	Minimum detection limit (MDL)
H_2O	0.5-5 %	
CO_2	0.35-15 %	
CO	0.035-1.5 %	
CF_4	0.5-150 ppmv	0.01 ppmv
C_2F_6	0.05-3.5 ppmv	0.03 ppmv
SF_6	0.5-5 ppmv	0.005 ppmv
SO_2	15-250 ppmv	1 ppmv
COS	0.5-15 ppmv	0.05 ppmv
HF	10-500 ppmv	0.05 ppmv

A total of 143 spectra were used when building the model. Most of these spectra were single component, spanning the relevant concentration range. A small subset of spectra was used for model validation. PLS calibration models were established for almost all components. Some of the components, CO (high concentrations only) and COS as well as CO_2 and H_2O, shared models. In some cases, models were built for specific concentration ranges. The ProtIR operation software allows for implementation of logic, where models can be selected in accordance with current component concentration level estimated.

Extractive FTIR monitoring of raw gas was performed before the eight dry scrubbers of a full smelter line. The gas was extracted through a 20 meter ¼" teflon tube, heated to 180 °C. Before instrument entry, the raw gas was filtered through a 47 mm ∅ particle filter (EMFAB TX40 IH20 WW) and a 37 mm ∅ KOH impregnated filter (Versapor 800 0.8 µm). The sampling rate was 2.5 nLpm. The same filters were used on four sampling locations. After approximately 30 minutes of sampling at each location, the sampling was repeated with five minute unfiltered measurements.

Open Path FTIR measurements were conducted by setting up a light path along the cell. This was made possible through a hatch opposite the door. The height profile of the light path was 30 cm near the hatch and 130 cm at the open door. The path was aimed along the line of feeders.

Results

The performance of the potassium hydroxide impregnated filters can be evaluated by looking at the hydrogen fluoride break-through concentration. This is illustrated in Figure 1.

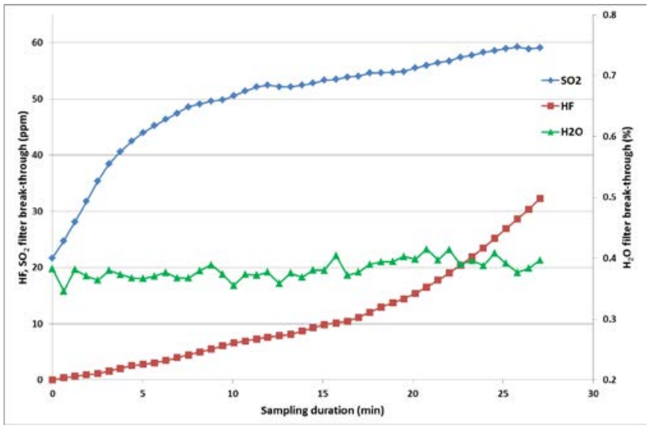

Figure 1. Break-through concentration profiles for HF, SO_2 and water on a fresh filter (filter 4).

When comparing the SO_2 and water estimates across filters, the effect observed in Figure 1 becomes obvious. From Figure 2 it can be seen that the first filter deviates most from its unfiltered SO_2 estimate than the remainder of the filters. Further, the fresh filters also show large deviation from the three other samplings conducted.

The unfiltered SO_2 concentration estimates represent the variation of both the FTIR sampling and quantitation as well as the process variations. In this case, the dilution of the raw gas may vary with fan power of the system. From Figure 2 it can be seen that the variation in SO_2 concentration is much higher than for the unfiltered measurements.

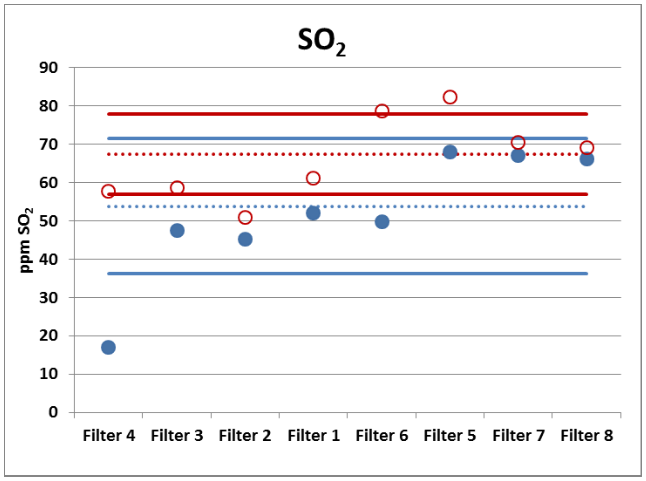

Figure 2. SO_2 filter break-through (blue, filled dots) and unfiltered (red, open dots) measurements. Mean (dotted line) and ± 1 standard deviation (solid lines) are indicated. Filters 4 and 6 were freshly installed.

In Figure 3, the changes in water break-through compared for filtered and unfiltered quantitation. A clear trend is observed for both fresh filters: water break-through decreases with time. As can be seen from the figure, the variation in the filtered measurement is much larger than for unfiltered measurements. There is also a complete opposite trend observed for the two fresh filters: the first matches the unfiltered reading initially, whereas the second matches the last unfiltered reading.

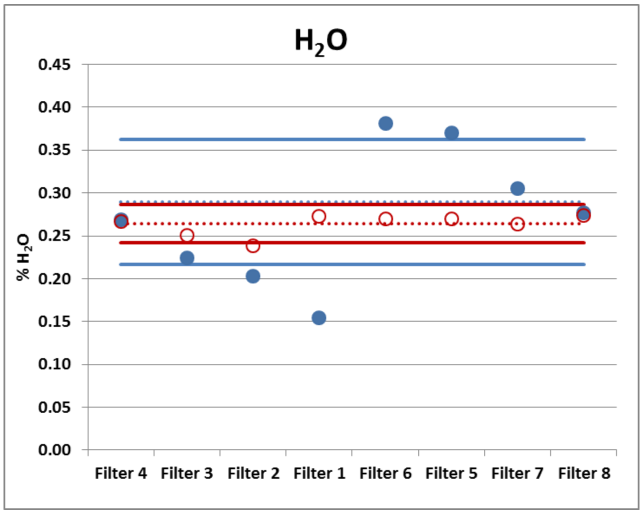

Figure 3. H_2O filter break-through (blue, filled dots) and unfiltered (red, open dots) measurements. Mean (dotted line) and ± 1 standard deviation (solid lines) are indicated. Filters 4 and 6 were freshly installed.

It appears that as the water content of the filter increases as it retains more water. The mechanism is not fully understood. A heated filter holder might have counteracted the effect on water filtration.

The results for the filtered and unfiltered readings of five gas gas components are summarized in Table 2. The correlations between filtered and burst measurements are good for CO and CO_2. For COS, the difference between filtered and unfiltered measurements is moderate: very low with the exceptions of filters 6 and 5. The variance in filtered (rsd 22 %) and unfiltered (rsd (18 %) are of the same magnitude. The variance is believed to originate either in process variation or quantitation.

Table 2. Averaged gas concentrations for all eight filters. Concentrations in ppmv or % vol. For SO_2, estimates where the values for fresh filters have been excluded are given in parenthesis.

	CO ppm	SO_2 ppm	COS ppm	H_2O %	CO_2 %
Filtered mean	764	54 (58)	6.3	0.29	0.79
SD	50	18 (11)	1.4	0.07	0.07
RSD	7 %	33 (18) %	22 %	24 %	9 %
Unfilt. mean	755	67	6.8	0.26	0.77
SD	32	10	1.2	0.02	0.09
RSD	4 %	15 %	18 %	8 %	12 %
Diff (%)	1.2	-22 (-14)	-7.3	9	2.9

Returning to SO_2, about half the variation observed for filters can be removed with the two fresh filters. The RSD for filtered versus unfiltered is then of comparable magnitude. There is still a significant difference in the SO_2 concentration estimates. When removing the two fresh filters, the difference is 14 %. As seen from Figure 1, the SO_2 filter break-through is fairly stable in the last half of the sampling interval. The establishment of a correction factor could be used for better estimation of the SO_2 concentration. As already mentioned, the variance in water filter break-through is high. The difference between filtered and unfiltered measurements is 9 %. A positive error suggests that water accumulation in the filter contributes positively to the break-through water concentration.

In order to justify the use of relatively short sampling times for unfiltered measurements, assessment of the instrument response times was evaluated. For the experimental setup used, 90 % signal of a 5 ppmv CF_4 standard was achieved in slightly more than two minutes. In Figure 4, the FTIR concentration profiles for four consecutive sampling locations are shown in Figure 4.

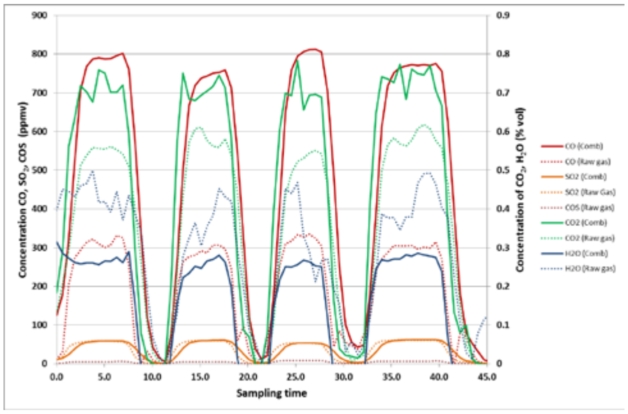

Figure 4. Concentration profiles for unfiltered sampling. Concentration estimates from Combustion model (solid lines) as well as the custom raw gas model (dotted lines). In between sampling locations, air was sampled.

From the figure it can be seen that the concentration levels stabilizes quickly, and that a five minute sampling period should be sufficient for a quantitative representation of the gas composition. The figure indicates that there is a large variation in the concentration estimates from the two calibration models. Especially CO, CO_2 and H_2O estimates are large. SO_2 estimates are fairly identical.

FTIR instrument validation is normally performed by sampling of a calibration gas of relevant composition. For complex gases, this is less feasible. Calibration gases are very often dry. Water has a very complex absorption spectrum in the IR range and should be present in the calibration gas as would be the case in the establishment of calibration models. As FTIR quantitation involves modeling, the concentration estimates are accompanied by parameters that give indication on "goodness of fit" for the model. In this case, the Relative Sum of Squares (RSS) has been used. The RSS parameters for the concentration estimates seen in Figure 4 are shown in Figure 5.

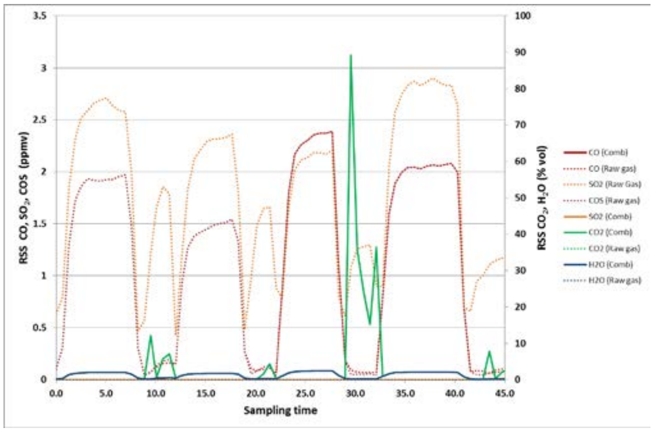

Figure 5. Concentration profiles for unfiltered sampling. Concentration estimates from Combustion model (solid lines) as well as the custom Raw gas model (dotted lines). In between sampling locations, air was sampled.

Figure 5 shows large RSS values for CO_2 (Combustion model) and SO_2 (Raw gas model). This is an indication of failure to model components when water concentration is low; a spectral range with contribution from water is used to quantify these components. For the four sampling locations, particularly the RSS of SO_2 (Raw gas model) as well as CO and COS (Raw gas model) and H_2O (Combustion model), display large RSS values. For SO_2 it can be seen from Figure 4 that the concentration estimates are almost identical. For H_2O, the higher estimate from the Raw gas model is given more credibility due to the lower RSS values. For CO, a very large discrepancy is observed between the two model concentration estimates. The Raw gas model also displays large RSS values, indicating failure to model CO well. Interestingly, Figure 5 shows that the RSS values of both CO and COS are coincidental. In order to explore this interaction further, calibration spectra of CO, COS as well as combined spectrum is shown in Figure 6. As can be seen from the figure, there is spectral overlap between the two components. Whereas this would pose a challenge for univarite calibration methods like Classic Least Squares (CLS), this is not an obstacle for the multivariate PLS approach. Quite the contrary: a shared model was chosen for CO and COS for simplicity. The shared RSS values is, however, an indication of an error in the model building.

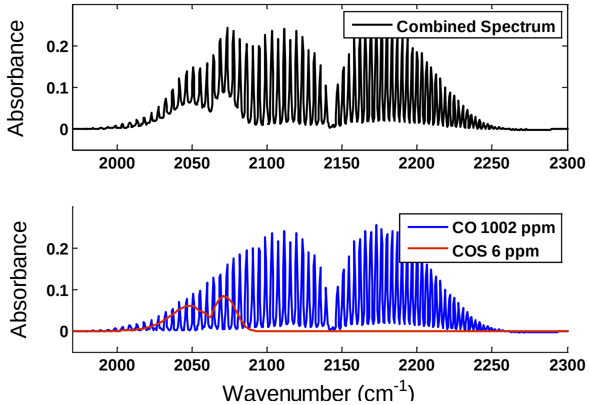

Figure 6. Relevant wavenumber range used for quantitation of CO and COS. In addition to a combined spectrum (top), individual calibration spectra for CO (1002 ppm) and COS (6 ppm) (botton) is overlaid to illustrate overlap in spectral range.

With the lack of a trustworthy RSS value for the COS concentration estimate, SINTEF did manual calculation of the CO and COS concentrations. For the sampling period in question a maximum concentration of 700 ppm for CO was estimated. This suggests that the CO estimate from the Combustion model is fairly good, but far better than the Raw gas estimate. As for the COS concentration, an estimate of 5.7 ppm was found. This suggests that although the RSS value is high, this has little impact on the concentration estimate.

Generally, it was found that the Combustion model was found to have better performance than our custom built Raw gas model. Set aside the error in CO and COS estimates, the CO_2 and H_2O concentration estimates are found to be generally better for the Combustion model. The reason is clear: the Combustion model is a well-established model that has undergone many revisions. These revisions make the model more robust. Our custom Raw gas model could improve significantly in one or two revisions. This illustrates well some of the challenges with multi component analyzers: more effort has to be put into the quantitation. Unlike the TDL single component analyzers, where concentration readouts are direct and fairly reliable given drift compensation, more effort has to be put into the quantitation. It is, however, certainly possible to obtain robust models for monitoring of the raw gas composition, given HF is removed.

The assessment of labile or non-extractive raw gas components has to be performed with open path instrumentation. Some of these gases include COF_2, CS_2, H_2S, SO_3, H_2SO_4. The easiest approach is probably to setup a light path across the duct much like TDL single component analyzers are installed. Another possibility is to beam across an electrolysis cell directly. The main challenge with this approach is the strong magnetic field: there are moving parts in the Michelson interferometer that might be affected. The through-cell Open-Path instrument setup is shown in Figure 7.

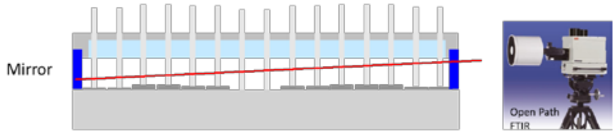

Figure 7. Through-cell setup for Open Path spectroscopy.

The motivation for the measurement was to evaluate possible assessment of Acid Dew Point (ADP) in the raw gas. As the effective conversion of SO_2 to SO_3 is not known, a sulphuric acid dew point of 40 to 80 °C was assumed. By using equations that correlate ADP with SO_3 concentrations [7, 8], an expected concentration of SO_3, given water concentration in air draught, could be found. SO_3 is very hygroscopic and below 400 °C efficiently forms sulphuric acid. This is not a challenge for the open path FTIR configuration as both species have unique spectra.

The results from this experiment gave no indication of sulphur gas species other than SO_2 and COS. The instrument expected sensitivity for SO_3 should be sufficient to detect a concentration equivalent to a dew point of 40 °C.

A benefit of open path spectroscopy is the dynamics. With a fast spectrometer, very fast changes in gas composition can be detected. In an electrolysis cell, the main challenge for the measurement is dust. As duct both absorb and emit light not to mention physical blocking of the light path, this can result in very noisy readings. The light path was aligned across the feeder holes in order to capture emitted species from openings in the crust. During feeding, a lot of noise was observed in the spectra. Feeding of alumina to the cell was therefore stopped. This resulted in more stable spectra. Inevitably, an anode effect occurred. Concentration profiles of some gas species is shown in Figure 8 [6].

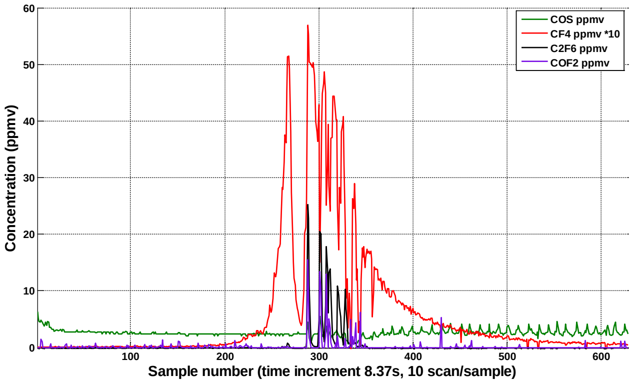

Figure 8. Through-cell Open Path FTIR spectroscopy concentration profiles for selected gas species.

As can be seen from the COS concentration profile, the noise level is much reduced when comparing the signal before and after the anode effect, when alumina feeding is again commenced. During the anode effect, the cell atmosphere was very noisy. Forced suction was also enabled when the anode effect was enabled, doubling the air draught. The quantitation of CF_4 was complicated by the saturation of signal at 1280 cm^{-1}. An early shoulder to the CF_4 signal is clearly observable. An offset in time between CF_4 and C_2F_6 is also observed. This is probably due to the fact that only CF4, illustr No trace of C3F8 was found in these measurements,. Expected concentrations are less than 20 % of C_2F_6 [10] and sufficient sensitivity for this component has not been verified. Interestingly, COF_2 was clearly present in these measurements at concentration levels comparable to those of C_2F_6. While COF_2 has been detected in laboratory scale setups with inert atmosphere, its presence in raw gas is unlikely due to hydrolysis:

$$COF_2 + H_2O = CO_2 + 2HF$$

In this experiment it plausible that COF_2 be present in the light path before reaction with water. There are several competing reactions, HF formation for one, which could render hydrolysis of COF_2 less efficient.

Monitoring of fugitive emissions was attempted by the application of Open Path FTIR monitoring. On the roof of a smelter, a 46 (2x23) meter path was setup as shown in Figure 9.

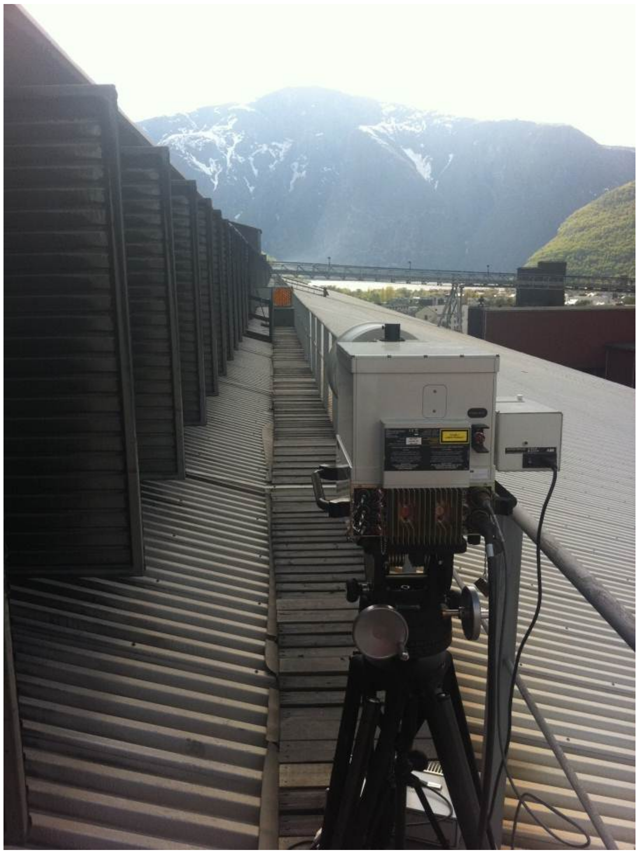

Figure 9. Open Path FTIR spectroscopy setup for fugitive emisision monitoring.

A collimating mirror is used to reflect light back to the detector. According to beers law, absorbance is a linear function of path length. Previous testing has indicated that when path lengths exceed 50 meters, distortion of signal is observed. Strategically, the path was placed across a sampling point where the smelter collects data for HF and SO_2 emissions. Data from a three day sampling period was compared to a 1.5 hour monitoring interval. For HF, the monitoring gave an average HF concentration of 1.3 ppmv whereas the sampling average was 0.5 ppmv. For SO_2, the monitoring average was 122 ppbv whereas sampling gave an average of 120 ppbv.

In order to evaluate the possibility of monitoring PFC emissions, an anode effect was ordered, by cancelling of alumina feeding, for an electrolysis cell just below the open path setup on the roof. As can be seen from Figure 10, the anode effect is easily detected by the roof instrument. The CF_4 concentration, a maximum of 450 ppbv was estimated is approximately 10 % of the concentration found after the dry scrubber on the train of 100 cells. Quantitation of PFC is therefore better performed after the dry scrubber.

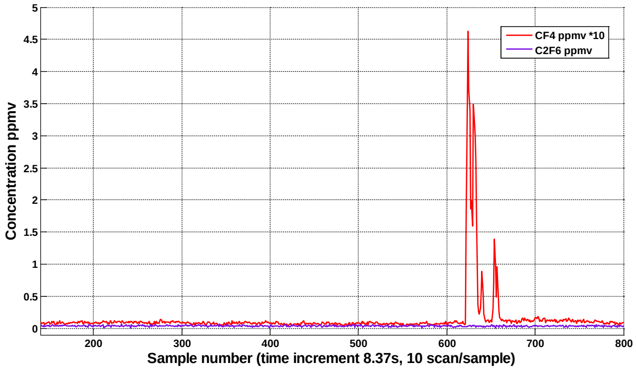

Figure 10. PFC concentration profiles for fugitive emissions monitoring.

Conclusions

Multicomponent analyzers provide some interesting opportunities when it comes to monitoring of gas from aluminium primary production. The drawbacks are high instrument cost as well as tolerance for HF for extractive gas monitoring. Some of the gas components can be monitored after the dry scrubber, and corrections for losses across the scrubber can be made. When monitoring of raw gas from single-, or a limited number of cells is required filtration of HF can be performed by hydroxide impregnated filters. During relatively short, a few hours, these filters can retain HF while other components pass the filter. Some losses in SO_2 can be compensated for as the break-through concentration show a logarithmic response with time. Open path monitoring of gas shows some interesting possibilities when it comes to qualification and quantification of labile species. Quantitation of quantitation models for multiple gas components is fairly simple with the appropriate software tools. The models provide residual values that can be used to evaluate the goodness of the concentration estimate. These models do however require some revision after intitial application.

Acknowledgement

This study is a part of the ROMA research project with financial support of the Research Council of Norway and Norwegian aluminium and metallurgical industry.

References

1. Ladam, Y., et. al, Light Metals, 2011, pp. 393-398.
2. Dando, N. and Lindsay, S., Light Metals 2008, pp. 227-232.
3. Gaertner, H. PhD dissertation, NTNU, 2013 (in press).
4. Grams IQ manual, Thermo Scientific.
5. NEO Lasergas II instrument for HF/H2O monitoring.
6. Aarhaug, T.A et al. Australasian Aluminium Smelting Technology Conference proceedings, 2011.
7. Verkhoff, F.H. and Banchero, J.T., Chem. Eng. Prog., 70 (8) 71 (1974).
8. Okkes, A.G. and Badger, B.V., Hydrocarbon Proc., 66 (7) 53 (1987).
9. Dorreen, M. et. al. Light Metals 1998, pp. 311-316.

10. Fraser, P. et al, Presentation at ESRL Global Monitoring Annual Conference, Boulder , Colorado, 13-14 May, 2009.